Preparation and characterization of WO$_3$/TiO$_2$ composite catalysts for the photoreduction of chromium(VI) in aqueous solutions

Simona Ostachavičiūtė*,

Eugenijus Valatka

*Department of Physical
and Inorganic Chemistry,
Kaunas University of Technology,
Radvilėnų Rd. 19,
LT-50254 Kaunas,
Lithuania*

Several WO$_3$/TiO$_2$ composite photocatalysts were prepared by impregnation of metatitanic acid in an aqueous solution of ammonium paratungstate (APT). The obtained photocatalysts were characterized by DSC-TG analysis, X-ray diffraction analysis and Fourier transform infrared spectroscopy. The photoreduction of potassium dichromate was used as a model reaction to evaluate the photocatalytic activity of prepared catalysts. The influence of methanol on the rate of photoreduction was also investigated. It was determined that the most active catalyst is obtained when the initial ratio of APT/TiO$_2$ is 1:4 and uncalcined metatitanic acid is used as a raw material for titania.

Key words: photocatalysis, composite photocatalyst, tungsten trioxide, titanium dioxide, impregnation

INTRODUCTION

Scientific community still exhibits a great interest in photocatalytic processes such as hydrogen generation during water photosplitting [1–4], photooxidation of organic substances [5–8] and even the removal of harmful inorganic materials [9–13]. Since Fujishima and Honda first published the results showing the photoelectrochemical activity of TiO$_2$ [14], various semiconductors (ZnO, WO$_3$, CdSe, etc.) were examined in the field of photocatalysis, yet titania still remains to be the most suitable for practical applications. TiO$_2$ has a strong oxidation ability and superhydrophilicity, it is a stable, nontoxic and inexpensive material. However, using it as a photocatalyst still has some major issues: due to the fast recombination of photogenerated charge carriers, the overall quantum efficiency is relatively low, and titania is mostly sensitive to the UV range spectrum. Different approaches may be taken to resolve these problems: nano-sized semiconductor crystal-lites can be used instead of bulk materials [15–17], the photocatalyst may be doped with various elements [18–21] or combining different semiconductors into one photocatalyst [22–26].

Tungsten trioxide is another semiconductor which can be employed in photocatalysis. Besides its photochromic properties, it has a smaller band gap than titania and may be activated under visible light illumination [27–31]. In order to improve the photocatalytic efficiency it may be reasonable enough to combine both titania and tungsten trioxide into one photocatalyst. Composite WO$_3$/TiO$_2$ catalysts have been reported to be prepared via various methods: impregnation [32, 33], flame synthesis [34], sol-gel method [35–37], electrochemical deposition [38–41] and even mechanical method [42]. The results obtained from these researches are mostly positive: bi-component tungsten trioxide and titania materials have shown enhanced photocatalytic and photoelectrocatalytic activity in comparison with their single component analogues due to the reduction of the charge carriers recombination. As this semiconduc-

---

* Corresponding author. E-mail: simona.ostachaviciute@ktu.lt

tor system was studied mostly in case of the photooxidation of organic substances, its potential to participate in the removal of inorganic harmful materials still needs to be explored.

It is now well established that Cr(VI) is one of the major pollutants in wastewater, usually from industrial processes such as paint production, leather tanning or electroplating. Chromium(VI) is highly toxic, carcinogenic and mutagenic and must be decontaminated. The preferred treatment is the reduction of Cr(VI) to Cr(III) upon the addition of sodium thiosulfate, ferrous sulfate, sulfur dioxide gas or sodium bisulfate / metabisulfite. Afterwards, Cr(III) ions can be precipitated as $Cr(OH)_3$. However, these methods require extensive use of chemicals. Numerous papers show that heterogeneous photocatalytic reduction may be used as an alternative [11, 43–48].

The aim of the current work was to produce new WO_3/TiO_2 composite photocatalysts via impregnation method and to study their photocatalytic activity towards the photoreduction of Cr(VI) ions. Kinetics of Cr(VI) photoreduction was also examined in the presence of organic compounds, which provide some insights about photoredox properties of the photocatalysts. This information is very important in the search of highly efficient photocatalysts suitable for various processes, such as water photo-splitting or oxidation of organic compounds.

EXPERIMENTAL

Preparation of composite WO_3/TiO_2 photocatalysts

As a raw material of titania, either metatitanic acid (H_2TiO_3, Reachim, Russia, 99% purity) or the T400 photocatalyst obtained by thermal decomposition of metatitanic acid for 1 h at 400 °C was used. The WO_3/TiO_2 catalysts were prepared according to the following procedure. Firstly, the powder of metatitanic acid or the T400 photocatalyst was stirred in an aqueous solution of ammonium paratungstate $((NH_4)_{10}W_{12}O_{41} \cdot n\ H_2O$, Reachim, Russia, further in the text denoted as APT) for 4 h at 80 °C. Afterwards the water was evaporated, samples were dried for 1 h at 110 °C, then calcined for 3 h at 600 °C under air atmosphere, thus obtaining a composite WO_3/TiO_2 catalyst. More detailed information is provided in Table 1.

Analytical techniques

The changes in the concentration of potassium dichromate were determined with a Perkin Elmer Lambda25 spectrometer by measuring the absorption at 352 nm wavelength.

The photoactivity of different catalyst samples was quantified in terms of the fractional conversion X of dichromate:

$$X = \frac{C_0 - C_t}{C_0} \cdot 100\%, \tag{1}$$

where C_0 and C_t are concentrations of potassium dichromate at the initial stage of the reaction and at the time t, respectively.

The photoactivity tests were carried out using a thermostated annular glass photoreactor containing 50 mL of the stirred aqueous suspension of dichromate and a catalyst. For all experimental runs, performed at 25 °C, the initial concentration of the photocatalyst was 5 gL^{-1}. The initial concentration of potassium bichromate ($K_2Cr_2O_7$, Reachim, Russia, 99%) was 0.25 mM. A 400 W high pressure metal halogen lamp (Philips 400/30S) was used as a source of UV irradiation and fixed outside the reactor. The incident light intensity was evaluated by potassium ferioxalate actinometry [49] and was found to be $9 \cdot 10^{18}$ photons/s in the range of 300–430 nm. The influence of methanol (CH_3OH, Penta, Czech Republic, 99.8%) concentration on the rate of photoreduction was investigated too. All experiments were carried out in the acid medium with the addition of 100 mM nitric acid (HNO_3, 65%, Penta, Czech Republic) to the suspension.

The X-ray powder diffraction (XRD) data were collected with a DRON-6 (Bourevestnik Inc., Russia) powder diffractometer with Bragg–Brentano geometry using Ni-filtered CuK$_\alpha$ radiation and a graphite monochromator. The crystallite size D_{hkl} was calculated from the line broadening using the Scherrer's equation [50]:

$$D_{hkl} = \frac{k \cdot \lambda}{B_{hkl} \cdot \cos\theta}, \tag{2}$$

where λ is the wavelength of the Cu K$_\alpha$ radiation (1.54056×10^{-10} m), θ is the Bragg diffraction angle, B_{hkl} is the full width at the half maximum intensity of the characteristic reflection peak, radian ($2\theta = 25.3°$ for anatase, $2\theta = 27.5°$ for rutile and $2\theta = 24.3°$ for tungsten trioxide) and k is a constant (the value used in this study was 0.94).

Table 1. **Synthesis conditions for various photocatalysts**

Sample number	Amount of WO_3 in the catalyst, wt. %	Raw material of TiO_2 used for impregnation	Denotation
1	7.2	H_2TiO_3	*W-TiO₂-1*
2	14.9	H_2TiO_3	*W-TiO₂-2*
3	26	H_2TiO_3	*W-TiO₂-3*
4	31.9	H_2TiO_3	*W-TiO₂-4*
5	7.2	T400	*W-T400-1*
6	14.9	T400	*W-T400-2*
7	26	T400	*W-T400-3*
8	31.9	T400	*W-T400-4*

The amount of rutile in the prepared catalyst was evaluated using the following equation [51]:

$$x = \left(1 + 0.8\frac{I_A}{I_R}\right)^{-1}, \qquad (3)$$

where x is the amount of rutile in TiO₂ particles, I_A and I_R are the maximum intensity of the characteristic reflection peak of anatase and rutile, respectively.

Fourier transform infrared (IR) absorption analysis was performed on a Perkin Elmer FT-IR System (Perkin Elmer, USA). A vacuum mold was used to form a tablet (1 mg of substance mixed with 200 mg of KBr). The analysis was performed in the range of 4 000–400 cm⁻¹.

Differential scanning calorimetry and thermogravimetry (DSC-TG) analysis was performed on a Netzsch STA 409 PC Luxx (Netzsch GmbH, Germany) simultaneous thermal analyzer. The heating was carried out in nitrogen atmosphere, the rate of temperature increase was 15 °C min⁻¹, and the temperature range from 30 to 650 °C was used.

Atomic absorption spectroscopy analysis (AAS) was performed with an AAnalyst 400 (Perkin Elmer, USA) spectrometer. Tungsten content was determined by measuring the absorption at the wavelength of 268.14 nm.

RESULTS AND DISCUSSION

Structural characterization of prepared WO₃/TiO₂ photocatalysts

It was previously established [52] that the T400 photocatalyst (a catalyst prepared via thermal decomposition of metatitanic acid at 400 °C for 1 h) is more effective than the commercial Degussa P25 TiO₂ which is often used as the standard to evaluate the activity of new UV light sensitive photocatalysts. For this reason we used metatitanic acid and T400 powders for impregnation. XRD patterns of some newly prepared WO₃/TiO₂ photocatalysts are presented in Fig. 1. They show that impregnation was successful and the final product does have tungsten trioxide in its structure. XRD data reveals that titania in the *W-T400-4* photocatalyst is composed of 70.6% rutile and 29.4% anatase, *W-TiO₂-4* is composed of 59.9% rutile and 40.1% anatase, and *W-TiO₂-2* is composed of 72.9% rutile and 27.1% anatase, as it is calculated by Equation (3). According to the Scherrer equation the average crystallite size of anatase and rutile is 32 and 12 nm, respectively. The average crystallite size of tungsten trioxide in the composite catalyst is 18 nm, whereas in calcined ammonium paratungstate 36 nm.

FTIR spectra of the same samples are presented in Fig. 2. Absorption peaks at 525 and 545 cm⁻¹ correspond well to Ti-O and Ti-OH vibrations, which usually occur at 450–800 cm⁻¹ [13]. A broad absorption band (peak at 3 310 cm⁻¹) is associated with OH⁻ and molecular water molecules adsorbed on the surface of metatitanic acid. SO₄²⁻ groups found with the impurities of metatitanic acid cause multiple absorption peaks at 1 200–1 071 cm⁻¹ [53]. The intensity of these peaks decreases upon heat-treatment of metatitanic acid.

Uncalcined as-prepared samples show the absorption peak at 1 400 cm⁻¹, which appears as a result of deformation vibrations of NH₄⁺ [54]. The absorption band at 938 cm⁻¹ is characteristic of the stretching mode of the terminal W=O bonds and does not appear after calcination. Uncalcined
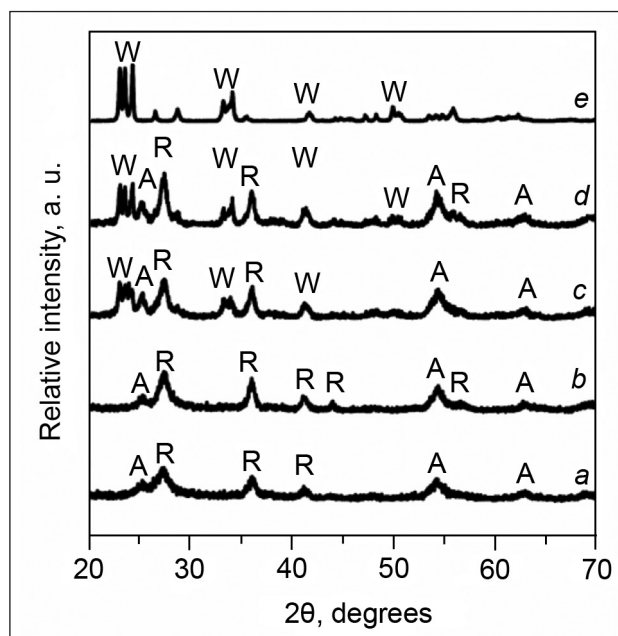
Fig. 1. XRD patterns of WO₃/TiO₂ catalysts: uncalcined samples of *W-TiO₂-4* (*a*) and *W-T400-4* (*b*); (*c*), (*d*), and (*e*) – samples of *W-TiO₂-4*, *W-T400-4* and ammonium paratungstate after calcination at 600 °C, respectively. Indexes: A – anatase, R – rutile, W – tungsten trioxide
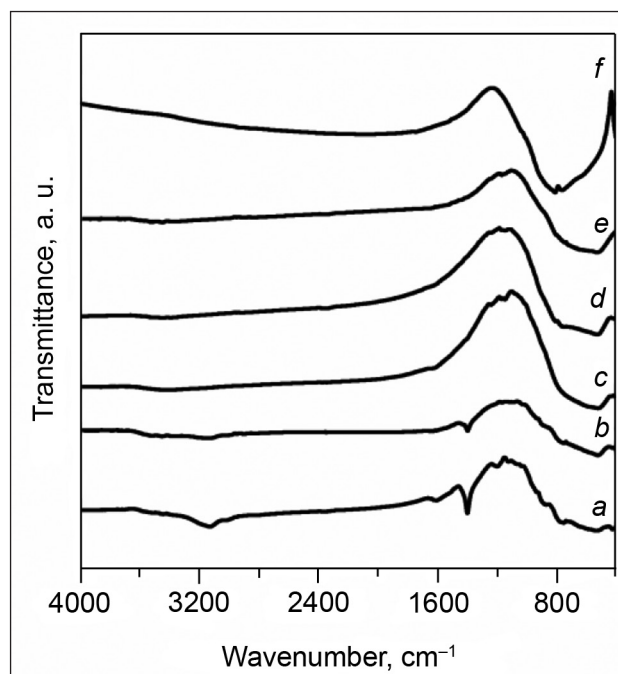
Fig. 2. FTIR spectra of TiO₂/WO₃ catalysts: uncalcined samples of *W-TiO₂-4* (*a*) and *W-T400-4* (*b*); (*c*), (*d*), (*e*) and (*f*) – samples of *W-TiO₂-2*, *W-TiO₂-4*, *W-T400-4* and ammonium paratungstate after calcination at 600 °C, respectively

samples also demonstrate the absorption band at 663 cm^{-1} corresponding to W-O stretching in amorphous WO$_3$. W-O stretching in crystalline WO$_3$ appears in all calcined samples at 750–850 cm^{-1}. Obtained data is in agreement with previous results in literature [55].

DSC-TG analysis was used to elucidate the structural changes of metatitanic acid (Fig. 3). Three endothermic effects at 93, 273 and 759 °C may be defined from the DSC curve and could be associated with the desorption of physically adsorbed water molecules, the loss of crystallization water and anatase transformation to rutile. Weight loss at the temperatures higher than 500 °C can be related to the decomposition of SO$_4^{2-}$ ions leading to SO$_3$ formation, followed by its decomposition into SO$_2$ and O$_2$ [56]. Data of the TG analysis shows the total weight loss of 16.8%, most of it is due to removal of physically adsorbed and crystalline water (~7.1 and ~5%, respectively).

The results of the DSC-TG analysis of ammonium paratungstate (Fig. 4) show that decomposition of APT proceeds in the steps described in literature [54, 57–60]. The first endothermic effect at 121 °C is related to the loss of a part of crystalline water (approximately two molecules). The second peak at 218 °C shows partial release of ammonia. The third endothermic effect at 283 °C is associated to the mutual liberation of ammonia and water. These results also show that ammonium paratungstate used for the experiment has 4 molecules of water. At the temperature higher than 500 °C no weight loss is observed in the TG curve.

DSC-TG analysis for the *W-T400-4* sample (Fig. 5) was performed in the temperature range of 30–600 °C, because higher temperatures have a detrimental effect on the photocatalytic activity of titania [52]. It shows only two endothermic effects, most likely to be associated with the loss of physically adsorbed water molecules, crystalline water and ammonia. The TG curve in Fig. 5 shows a monotonic weight

loss throughout the whole temperature range due to various ongoing processes of the metatitanic acid and APT decomposition (Figs. 3, 4), mostly related to the loss of water, ammonia and sulfate ions.

Photocatalytic activity of prepared WO$_3$/TiO$_2$ photocatalysts

Photocatalytic behavior of synthesized catalysts was determined through photocatalytic reduction of chromium(VI) in a thermostated annular glass photoreactor containing 50 mL of the stirred aqueous suspension of potassium dichromate, catalyst and nitric acid, which is needed to maintain the stability of tungsten trioxide.

As it is shown in Fig. 6, the *W-T400-4* catalyst is less active than T400. After 10 min of irradiation the fractional conversion of Cr(VI) ions is 85.2% (the concentration of dichro-
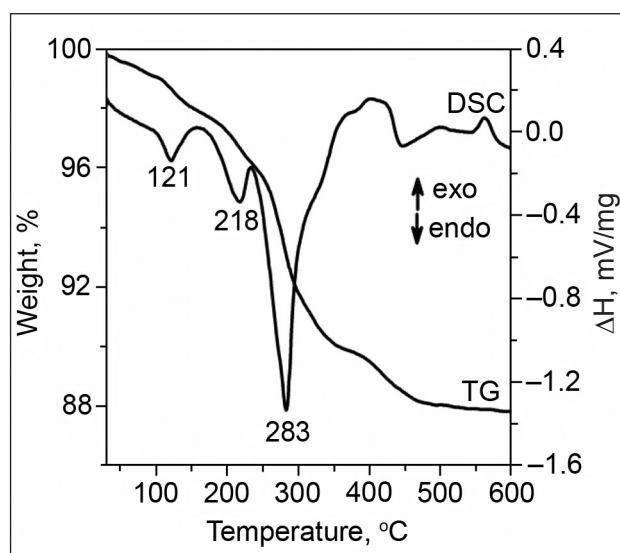
Fig. 4. TG–DSC curves of ammonium paratungstate
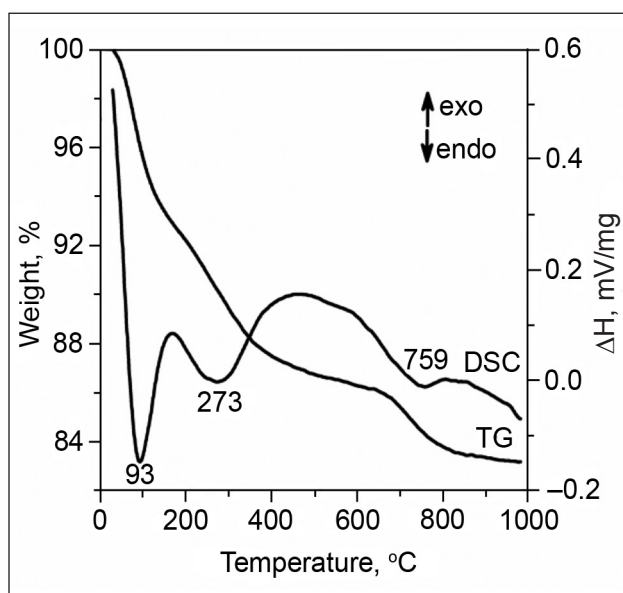
Fig. 3. TG–DSC curves of metatitanic acid
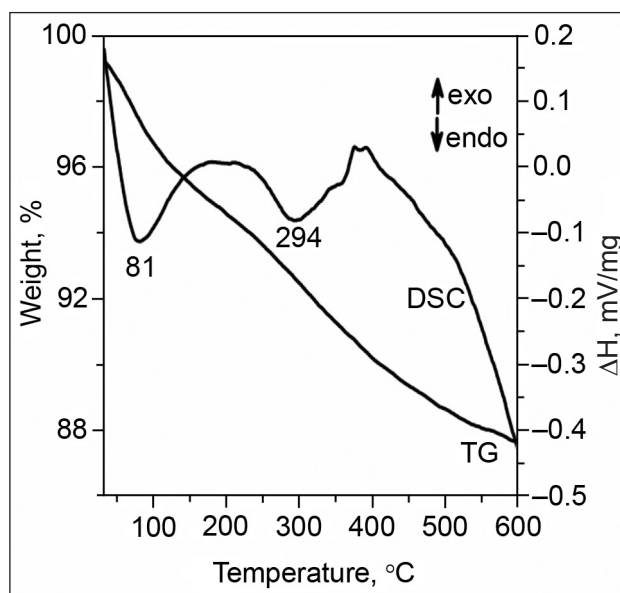
Fig. 5. TG–DSC curves of as-prepared *W-TiO$_2$-4* catalyst
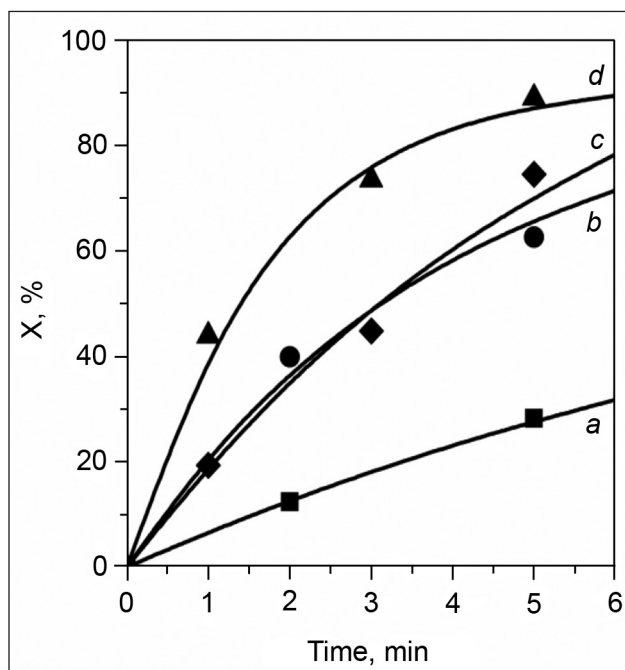
Fig. 6. Effects of methanol on Cr(VI) fractional conversion (X): *W-T400-4*, no methanol (*a*), T400, no methanol (*b*); *W-T400-4*, 5 mM of methanol (*c*), T400, 5 mM of methanol (*d*). Experimental conditions: t = 25 °C, $C^0_{K_2Cr_2O_7}$ = 0.25 mM, $C^0_{HNO_3}$ = 100 mM

mate decreased from 0.25 mM to 0.037 mM) for T400, and only 44.3% for *W-T400-4*. No changes in the chromium(VI) concentration were observed under irradiation in the absence of photocatalysts. It was determined [61, 62] that the photochemical reduction of Cr(VI) proceeds at appreciable rate only in strongly acidic solutions. The blank experiments revealed that the direct photolysis and chemical reduction of Cr(VI) do not present considerable contributions to the observed concentration variations under the used experimental conditions. Metatitanic acid H$_2$TiO$_3$ is characterized by a very low photocatalytic activity. The decrease in Cr(VI) concentration may be associated with photocatalytic redox processes occurring on the surface of the photocatalyst [7]. Under UV irradiation the generation of photoelectrons (e$^-$) and holes (h$^+$) takes place in the semiconductor particle. The interaction between photoelectrons e$^-$ and Cr$_2$O$_7^-$ ions may lead to the formation of Cr^{3+} ions [46]:

$$Cr_2O_7^{2-} + 14H^+ + 6e^- \rightarrow 2Cr^{3+} + 7H_2O. \tag{4}$$
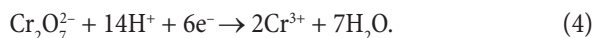
It is known that in aqueous solutions Cr(VI) ions can exist in several forms: H$_2$CrO$_4$, HCrO$_4^-$, Cr$_2$O$_7^{2-}$ or CrO$_4^{2-}$ depending on pH. Our experiments were carried out at an initial pH 1.3. On the basis of thermodynamic calculations [63], we presume that under such experimental conditions the reaction mixture consists of 87% HCrO$_4^-$, 10% Cr$_2$O$_7^{2-}$ and 3% CrO$_4^{2-}$. As a result, Equation (4) may be transformed to

$$HCrO_4^- + 7H^+ + 3e^- \rightarrow Cr^{3+} + 4H_2O. \tag{5}$$
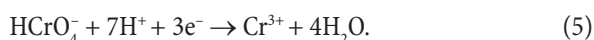
Photogenerated holes h$^+$ oxidize water molecules with a formation of ·OH radicals:

$$H_2O + h^+ \rightarrow ·OH + H^+ \tag{6}$$

or

$$2H_2O + 4h^+ \rightarrow O_2 + 4H^+. \tag{7}$$
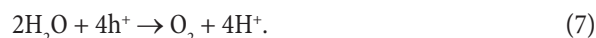
Hereby, chromium(VI) reduction to chromium(III) and oxygen release are the main processes in this system. At the kinetic point of view, these processes are slow, because more than one electron must be transferred.

It is generally accepted that reaction between photogenerated holes and water molecules (Equations 6 and 7) is the limiting stage of photocatalytic processes. Therefore, photogenerated charge carriers tend to recombine, thus, reducing the efficiency of photocatalysis. Recombination rate can be decreased by using organic additives which can be readily oxidized on the surface of the catalyst.

The rate of the photocatalytic reduction of potassium dichromate increases significantly (Fig. 6) with the addition of methanol, especially when the composite WO$_3$/TiO$_2$ catalyst is used. By comparing the results shown in Fig. 6 it is seen that the conversion of Cr(VI) after 10 min of irradiation increases from 85.2 to 91.8% for T400 and from 44.3% to 98.6% for *W-T400-4*. These results are in agreement with those obtained by other authors [12, 46, 64]. For example, in [46] the influence of different organic compounds (p-hydroxybenzoic acid, phenol, salicylic and citric acids) was studied. The positive influence was found for all organic additives; however, the effect depends on the nature of organic compound. In the case of citric acid the reduction rate constant increases more than 20 times. Wang et al. [64] determined that an addition of colorless organic acids resulted in the formation of a charge-transfer complex which is sensitive to visible light irradiation and induces the photocatalytic oxidation of organic acids and photoreduction of Cr(VI). Among the used acids, tartaric acid was found to be the most efficient.

Figure 7 demonstrates how the fractional conversion of chromium(VI) depends on the initial concentration of methanol. It shows that the *W-T400-4* photocatalyst reaches higher fractional conversion values than T400, when higher doses of methanol (more than 10 mM) are added to the suspension: after 5 min of irradiation up to 95.4% and 92.1% of hexavalent chromium are reduced to its trivalent form, when *W-T400-4* and T400 catalysts are used for the experiment.

During the experimental tests it was observed that particles of the composite catalyst acquire a dark blue color if methanol is present in the reaction medium. It could be due to the transformation of WO$_3$ to non-stoichiometric tungsten oxide WO$_{3-x}$ [65, 66].

Further experiments were performed using a suspension consisting of 0.25 mM potassium dichromate, 100 mM nitric acid, 5 mM methanol and 5 g/l of catalyst. All prepared
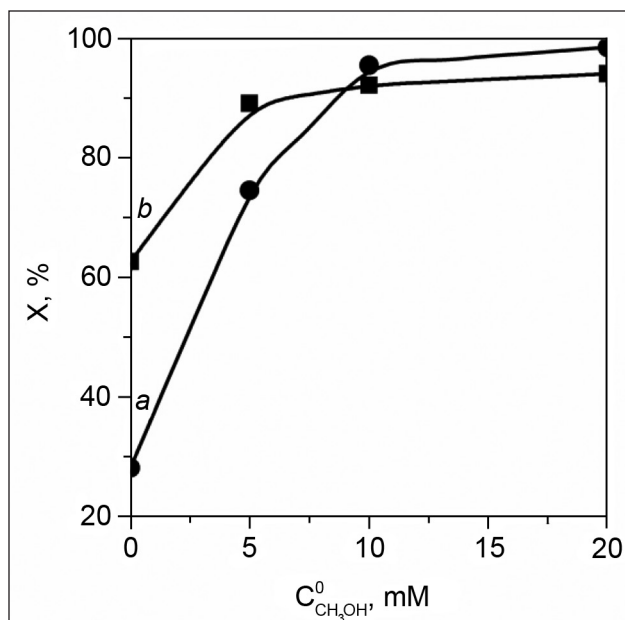
Fig. 7. Cr(VI) fractional conversion (X) as a function of initial concentration of methanol in the presence of *W-T400-4* (*a*) and T400 (*b*) photocatalysts. Experimental conditions: t = 25 °C, $C^0_{K_2Cr_2O_7}$ = 0.25 mM, $C^0_{HNO_3}$ = 100 mM, time 5 min
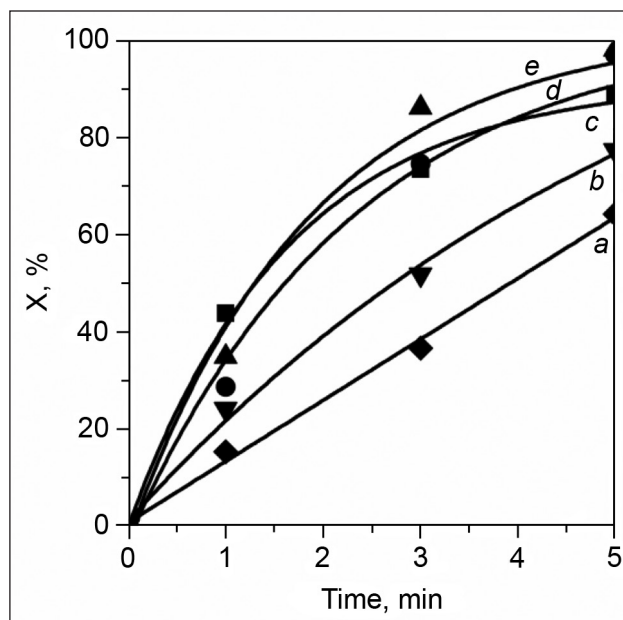
Fig. 9. Cr(VI) fractional conversion (X) as a function of time in the presence of different photocatalyst: *W-TiO$_2$-4* (*a*), *W-TiO$_2$-3* (*b*), T400 (*c*), *W-TiO$_2$-1* (*d*), *W-TiO$_2$-2* (*e*). Experimental conditions: t = 25 °C, $C^0_{K_2Cr_2O_7}$ = 0.25 mM, $C^0_{HNO_3}$ = 100 mM, $C^0_{CH_3OH}$ = 5 mM
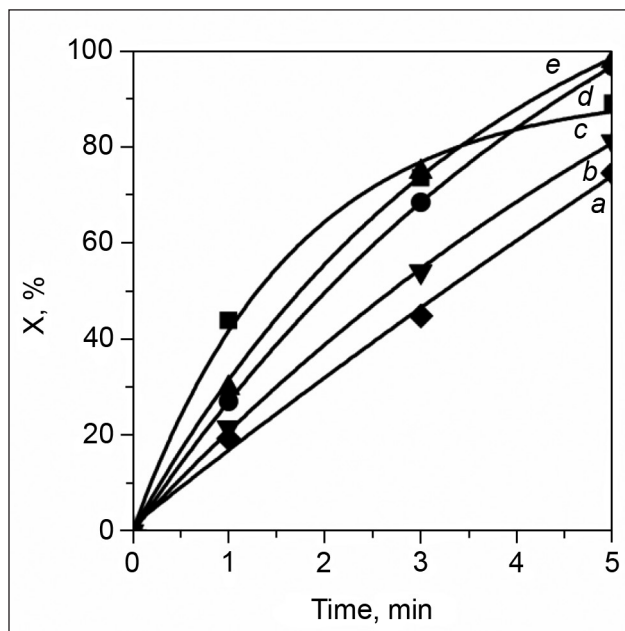
Fig. 8. Cr(VI) fractional conversion (X) as a function of time in the presence of different photocatalyst: *W-T400-4* (*a*), *W-T400-3* (*b*), T400 (*c*), *W-T400-1* (*d*), *W-T400-2* (*e*). Experimental conditions: t = 25 °C, $C^0_{K_2Cr_2O_7}$ = 0.25 mM, $C^0_{HNO_3}$ = 100 mM, $C^0_{CH_3OH}$ = 5 mM

samples were tested. The obtained data is provided in Figs. 8 and 9, splitting the results into two groups depending on what titania material was used for the impregnation: T400 (Fig. 8) or metatitanic acid (Fig. 9). It shows that the best photocatalysts are obtained when the initial ratio of APT/

TiO$_2$ is 1/4 (samples denoted as *W-TiO$_2$-2* and *W-T400-2*). Samples *W-TiO$_2$-1* and *W-T400-1* also have greater photocatalytic activity than T400 after only 3 min of irradiation. All composite WO$_3$/TiO$_2$ demonstrate to reach higher fractional conversion value (up to 98.7%) than T400 (thus also commercial Degussa P25) after 10 min of irradiation.

The comparison of all obtained catalysts is provided in Table 2. It shows how the fractional conversion of Cr(VI) changes depending on the catalyst at the same moment of time.

Kinetic data presented in Figs. 8 and 9 were used for the calculation of apparent reaction order (n) with respect to the potassium dichromate concentration. For this purpose, the plots of the logarithms of the photoreduction rates (v) against the logarithms of the bichromate concentrations (c) were constructed (Figs. 10, 11). The obtained results show that the value of the apparent reaction order (n) changes with the increase in the amount of tungsten oxide and varies in the range of 0–0.5, thus implying the changes of the mechanism of chromium(VI) photoreduction.

Stability of prepared WO$_3$ in acidic solutions

Tungsten oxide prepared by the thermal decomposition of ammonium paratungstate was tested for chemical dissolution in an acidic medium. Experiments were carried out in aqueous HNO$_3$ solutions of different pH at 25 °C. The initial amount of WO$_3$ was 20 gL^{-1}, which was mixed in the acidic solution for 3 h, then samples were drawn for tungsten content analysis. The experimental data reveals that tungsten oxide is stable at pH 1.3 and 2.6 even when irradiated with UV light. At pH 5.2 the amount of dissolved W was 139.8 mgL^{-1}.

Table 2. **Comparison of photocatalytic activity of WO₃/TiO₂ powders. Experimental conditions: t = 25 °C, $C^0_{K_2Cr_2O_7}$ = 0.25 mM, $C^0_{CH_3OH}$ = 5 mM, time 5 min**

Sample (as denoted)	Calcination temperature t, °C	Fractional conversion X, %
No catalyst	–	6.9
APT	400/600	56.3/62.1
T400	400	89
W-TiO₂-1	400/600	82/97
W-TiO₂-2	400/600	82.5/98.1
W-TiO₂-3	600	77.4
W-TiO₂-4	600	64.3
W-T400-1	400/600	79.8/96.5
W-T400-2	400/600	83.5/97.8
W-T400-3	600	81
W-T400-4	600	74.5
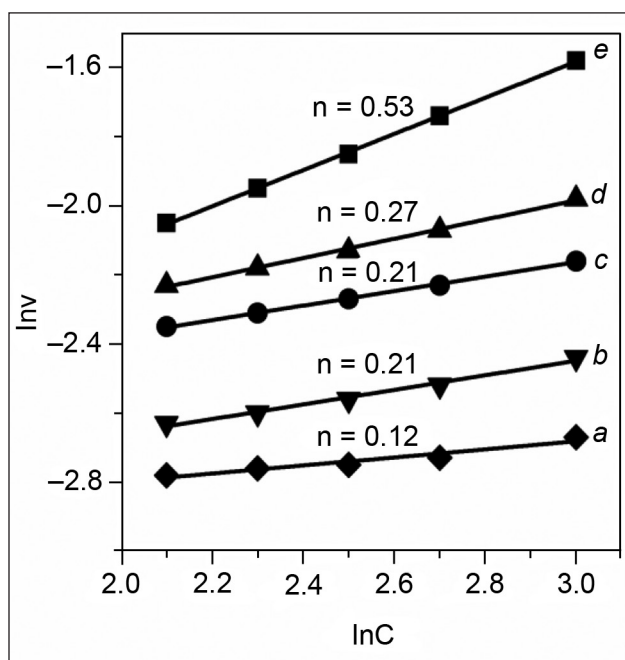
Fig. 10. Linear plots lnv = *f*(lnC) for calculation of apparent reaction order with respect to K₂Cr₂O₇ concentration for various photocatalysts: *W-T400-4* (*a*), *W-T400-3* (*b*), *W-T400-1* (*c*), *W-T400-2* (*d*), T400 (*e*)
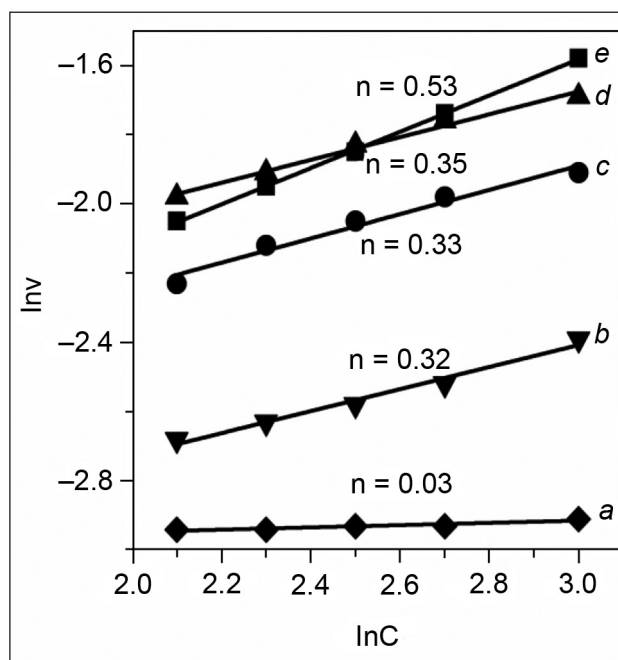
Fig. 11. Linear plots lnv = *f*(lnC) for calculation of apparent reaction order with respect to K₂Cr₂O₇ concentration for various photocatalysts: *W-TiO₂-4* (*a*), *W-TiO₂-3* (*b*), *W-TiO₂-1* (*c*), *W-TiO₂-2* (*d*), T400 (*e*)

CONCLUSIONS

WO₃/TiO₂ composite photocatalysts were prepared by impregnation of metatitanic acid or T400 catalyst in an aqueous solution of ammonium paratungstate, followed by calcination for 3 h at 600 °C in order for APT to decompose into tungsten trioxide. The experimental results revealed that the photocatalytic activity of WO₃/TiO₂ composite catalysts is highly affected by the composition of particles and the presence of organic additives in the suspension. It has been established that WO₃/TiO₂ catalysts are more active in the photoreduction of chromium(VI), if methanol is added to the suspension. Photocatalytic activity also depends on the initial ratio of (NH₄)₁₀W₁₂O₄₁ · n H₂O / TiO₂: the catalysts containing small amounts of tungsten trioxide were found to show the best performance at reducing chromium(VI). Additionally, stability of WO₃ in an acidic medium was tested which showed that our prepared catalysts are stable under experimental conditions.

References

1. R. Abe, *J. Photoch. Photobio. C*, **11(4)**, 179 (2010).
2. D. W. Jing, L. J. Guo, L. A. Zhao, et al., *Int. J. Hydrogen Energ.*, **35(13)**, 7087 (2010).
3. H. H. Yang, L. J. Guo, W. Yan, H. T. Liu, *J. Power Sources*, **159(2)**, 1305 (2006).
4. K. Maeda, *J. Photoch. Photobio. C*, **12(4)**, 237 (2011).
5. D. Bahnemann, *Sol. Energy*, **77(5)**, 445 (2004).

6. M. N. Chong, B. Jin, C. W. K. Chow, C. Saint, *Water Res.*, **44(10)**, 2997 (2010).

7. U. I. Gaya, A. H. Abdullah, *J. Photoch. Photobio. C*, **9(1)**, 1 (2008).

8. X. Z. Li, F. B. Li, C. L. Yang, W. K. Ge, *J. Photoch. Photobio. A*, **141(2–3)**, 209 (2001).

9. D. Chen, A. K. Ray, *Chem. Eng. Sci.*, **56(4)**, 1561 (2001).

10. V. N. H. Nguyen, R. Amal, D. Beydoun, *Chem. Eng. Sci.*, **58(19)**, 4429 (2003).

11. R. Vinu, G. Madras, *Environ. Sci. Technol.*, **42(3)**, 913 (2008).

12. D. D. Shao, X. K. Wang, Q. H. Fan, *Micropor. Mesopor. Mat.*, **117(1–2)**, 243 (2009).

13. S. Sajjad, S. A. K. Leghari, F. Chen, J. L. Zhang, *Chem.-Eur. J.*, **16(46)**, 13795 (2010).

14. A. Fujishima, K. Honda, *Nature*, **238**, 37 (1972).

15. A. J. Maira, K. L. Yeung, C. Y. Lee, P. L. Yue, C. K. Chan, *J. Catal.*, **192(1)**, 185 (2000).

16. J. F. Zhu, M. Zach, *Curr. Opin. Colloid. In.*, **14(4)**, 260 (2009).

17. A. Panniello, M. L. Curri, D. Diso, et al., *Appl. Catal. B-Environ.*, **121**, 190 (2012).

18. A. V. Vorontsov, I. V. Stoyanova, D. V. Kozlov, V. I. Simagina, E. N. Savinov, *J. Catal.*, **189(2)**, 360 (2000).

19. L. S. Yoong, F. K. Chong, B. K. Dutta, *Energy*, **34(10)**, 1652 (2009).

20. R. Dholam, N. Patel, M. Adami, A. Miotello, *Int. J. Hydrogen Energ.*, **34(13)**, 5337 (2009).

21. S. Bangkedphol, H. E. Keenan, C. M. Davidson, et al., *J. Hazard. Mater.*, **184(1–3)**, 533 (2010).

22. J. T. Tian, L. J. Chen, Y. S. Yin, et al., *Surf. Coat. Tech.*, **204(1–2)**, 205 (2009).

23. T. K. Ghorai, S. Pramanik, P. Pramanik, *Appl. Surf. Sci.*, **255(22)**, 9026 (2009).

24. C. Xu, L. X. Cao, G. Su, et al., *J. Hazard. Mater.*, **176(1–3)**, 807 (2010).

25. C. L. Yu, K. Yang, Q. Shu, et al., *Chinese J. Catal.*, **32(4)**, 555 (2011).

26. F. Wang, X. J. Chen, X. L. Hu, K. S. Wong, J. C. Yu, *Sep. Purif. Technol.*, **91**, 67 (2012).

27. G. R. Bamwenda, H. Arakawa, *Appl. Catal. a-Gen.*, **210(1–2)**, 181 (2001).

28. G. Waldner, A. Bruger, N. S. Gaikwad, M. Neumann-Spallart, *Chemosphere*, **67(4)**, 779 (2007).

29. S. J. Hong, H. Jun, P. H. Borse, J. S. Lee, *Int. J. Hydrogen Energ.*, **34(8)**, 3234 (2009).

30. H. Widiyandari, A. Purwanto, R. Balgis, T. Ogi, K. Okuyama, *Chem. Eng. J.*, **180**, 323 (2012).

31. W. Zhao, Z. Y. Wang, X. Y. Shen, et al., *Int. J. Hydrogen Energ.*, **37(1)**, 908 (2012).

32. A. Ulgen, W. F. Hoelderich, *Appl. Catal. a-Gen.*, **400(1–2)**, 34 (2011).

33. X. L. Yang, W. L. Dai, C. W. Guo, et al., *J. Catal.*, **234(2)**, 438 (2005).

34. K. K. Akurati, A. Vital, J. P. Dellemann, et al., *Appl. Catal. B-Environ.*, **79(1–2)**, 53 (2008).

35. A. K. L. Sajjad, S. Shamaila, B. Z. Tian, F. Chen, J. L. Zhang, *J. Hazard. Mater.*, **177(1–3)**, 781 (2010).

36. G. M. Zuo, Z. X. Cheng, H. Chen, G. W. Li, T. Miao, *J. Hazard. Mater.*, **128(2–3)**, 158 (2006).

37. H. Yang, D. Zhang, L. Wang, *Mater. Lett.*, **57(3)**, 674 (2002).

38. J. Georgieva, E. Valova, S. Armyano, et al., *J. Hazard. Mater.*, **211**, 30 (2012).

39. S. Somasundaram, C. R. Chenthamarakshan, N. R. de Tacconi, N. A. Basit, K. Rajeshwar, *Electrochem. Commun.*, **8(4)**, 539 (2006).

40. J. Georgieva, S. Armyanov, E. Valova, I. Poulios, S. Sotiropoulos, *Electrochem. Commun.*, **9(3)**, 365 (2007).

41. N. R. de Tacconi, C. R. Chenthamarakshan, K. Rajeshwar, T. Pauporte, D. Lincot, *Electrochem. Commun.*, **5(3)**, 220 (2003).

42. S. F. Chen, L. Chen, S. Gao, G. Y. Cao, *Powder Technol.*, **160(3)**, 198 (2005).

43. A. Watcharenwong, W. Chanmanee, N. R. de Tacconi, et al., *J. Electroanal. Chem.*, **612(1)**, 112 (2008).

44. N. S. Waldmann, Y. Paz, *J. Phys. Chem. C*, **114(44)**, 18946 (2010).

45. L. X. Yang, Y. Xiao, S. H. Liu, et al., *Appl. Catal. B-Environ.*, **94(1–2)**, 142 (2010).

46. L. M. Wang, N. Wang, L. H. Zhu, H. W. Yu, H. Q. Tang, *J. Hazard. Mater.*, **152(1)**, 93 (2008).

47. S. Chakrabarti, B. Chaudhuri, S. Bhattacharjee, A. K. Ray, B. K. Dutta, *Chem. Eng. J.*, **153(1–3)**, 86 (2009).

48. J. Kuncewicz, P. Zabek, G. Stochel, Z. Stasicka, W. Macyk, *Catal. Today*, **161(1)**, 78 (2011).

49. Z. Kulesius, Ph. D. Thesis, Kaunas University of Technology (2008).

50. L. V. Azaroff, *Elements of X-Ray Crystallography*, McGraw-Hill, New York (1968).

51. R. A. Spurr, H. Myers, *Anal. Chem.*, **29** (1957).

52. S. Mockunaite, S. Ostachaviciute, E. Valatka, *Chemija*, **23(3)**, 187 (2012).

53. L. Ge, M. X. Xu, *J. Sol-Gel Sci. Techn.*, **43(1)**, 1 (2007).

54. I. M. Szilagyi, J. Madarasz, F. Hange, G. Pokol, *Solid State Ionics*, **172(1–4)**, 583 (2004).

55. A. Cremonesi, D. Bersani, P. P. Lottici, Y. Djaoued, P. V. Ashrit, *J. Non-Cryst. Solids*, **345**, 500 (2004).

56. J. Winkler, *Titanium Dioxide*, Vincentz Network, Hannover (2003).

57. M. Fait, H. J. Lunk, M. Feist, et al., *Thermochim. Acta*, **469(1–2)**, 12 (2008).

58. M. J. G. Fait, H. J. Lunk, *Eur. J. Inorg. Chem.*, **(2)**, 213 (2012).

59. J. Madarasz, I. M. Szilagyi, F. Hange, G. Pokol, *J. Anal. Appl. Pyrol.*, **72(2)**, 197 (2004).

60. M. S. Marashi, J. V. Khaki, S. M. Zebarjad, *Int. J. Refract. Met. H*, **30(1)**, 177 (2012).

61. P. Mohapatra, S. K. Samantaray, K. Parida, *J. Photoch. Photobio. A*, **170(2)**, 189 (2005).

62. L. A. G. Rodenas, A. D. Weisz, G. E. Magaz, M. A. Blesa, *J. Colloid. Interf. Sci.*, **230(1)**, 181 (2000).

63. M. Alam, R. A. Montalvo, *Metall. Mater. Trans. B*, **29B**, 95 (1998).

64. N. Wang, L. H. Zhu, K. J. Deng, et al., *Appl. Catal. B-Environ.*, **95(3–4)**, 400 (2010).

65. R. Q. Cabrera, E. R. Latimer, A. Kafizas, et al., *J. Photoch. Photobio. A*, **239(0)**, 60 (2012).

66. A. Gupta, P. Ifeacho, C. Schulz, H. Wiggers, *P. Combust. Inst.*, **33(2)**, 1883 (2011).

Simona Ostachavičiūtė, Eugenijus Valatka

WO$_3$/TiO$_2$ MIŠRIŲ KATALIZATORIŲ SINTEZĖ, STRUKTŪRA IR TAIKYMAS CHROMO(VI) FOTOREDUKCIJAI VANDENINIUOSE TIRPALUOSE

Santrauka

Darbo metu mišrūs WO$_3$/TiO$_2$ katalizatoriai susintetinti impregnuojant metatitanato rūgštį arba iš jos amonio paravolframatu vandeniniuose tirpaluose pagamintą titano dioksidą. Gautųjų miltelių struktūrai charakterizuoti panaudota rentgeno spindulių difrakcinė analizė, diferencinė skenuojančioji kalorimetrija ir termogravimetrinė (DSK–TG) analizė bei infraraudonojo (IR) spektro molekulinė absorbcinė analizė. Fotokatalizatorių aktyvumas įvertintas kalio bichromato fotocheminės redukcijos reakcijoje. Nustatyta, kad paruoštų katalizatorių aktyvumas priklauso nuo volframo trioksido kiekio bei metanolio priedo tirtose suspensijose. Eksperimentiniai rezultatai atskleidė, kad didžiausias aktyvumas būdingas WO$_3$/TiO$_2$ milteliams, kuriuose WO$_3$ kiekis yra apie 15 % (masės). Remiantis eksperimentiniais duomenimis, apskaičiuotos dalinio reakcijos laipsnio kalio bichromato koncentracijos atžvilgiu vertės. Gauta, kad didėjant WO$_3$ kiekiui katalizatoriuje dalinio reakcijos laipsnio vertės mažėja nuo 0,5 iki 0. WO$_3$ tirpumo rūgštiniuose tirpaluose tyrimo rezultatai parodė, kad fotokatalizatoriai yra atsparūs fotokorozijai, jeigu vandeninės suspensijos pH < 3.